Prototype Tracking Simulation for Nuclear Power Plant Dismantling Using a BIM-Based Radiation Model

Hyong Chol Kim*, Jae Hee Ro, Moonjoo Gil, Young Jin Lee
NSE Technology, 5F Convergence Technology Research Commercialization Center
218 Gajeong-ro, Yuseong-gu, Daejeon, 34129, Republic of Korea
**Corresponding author: hckim@nsetec.com*

***Keywords:** source strength, dose rate, BIM, nuclear power plant, decommissioning, dismantling, tracking

1. Introduction

In recent years, 3D modeling techniques have become widely utilized in the design, operation, and decommissioning of nuclear power plants (NPPs). For NPP decommissioning, radiological characterization is conducted to gather information on the type, quantity, and distribution of radionuclides within the facility. A Building Information Modeling (BIM)-based program can be employed to determine the activity levels of radiation sources, enhancing both efficiency and safety in dismantling components and managing radioactive materials during decommissioning processes [1].

A virtual simulation system for radiation work processes is crucial in mitigating potential challenges and associated risks. 3D model-based dose assessment programs have been developed to support the 'As Low As Reasonably Achievable' (ALARA) analysis in radiation work planning [2,3].

Previously, a BIM-based software program called BIMRAD was introduced to determine radiation source strengths based on dose rates measured in the field [4]. This study aims to demonstrate how BIMRAD can be utilized for tracking simulations during an NPP dismantling process and to showcase its application in assessing the radiation field and radiation exposure during radiation-related tasks.

2. Methods

2.1 Determination of Source Strength from Field-Measured Dose Rates

The dose rate response term (R_{mj}) at position r_m, due to a source at position r_j with unit activity strength in Bq/cm^3 and volume V_j, can be expressed as a function of the distance between the source and the measurement point, as well as the path length through the medium, using the point kernel method [4].

The path length is determined by identifying pairs of coordinate points on the inlet and outlet surface meshes of the shielding object models where the line connecting the source to the measurement point intersects. The self-shielding length of the source is calculated algebraically by determining the intersection of the line extending from the center of each cell within the source model to the measurement point.

Let the source strength of source j be denoted as S_j. The dose rate (D_m) measured at position m can be expressed as the sum of contributions from all sources as follows:

$$D_m = \sum_{j=1}^{N}\left[R_{mj} \cdot S_j\right] \ (m = 1, \cdots, M; M \geq N) , \qquad (1)$$

where M is the number of measured points and N is the number of sources. It is assumed here that M is greater than or equal to N.

The set of inverse problem equations for S_j that satisfy Eq. (1) with the least square error can be expressed as follows:

$$\sum_{j=1}^{N}[(\textstyle\sum_{m=1}^{M} R_{mk} R_{mj}) \cdot S_j] \\ = \sum_{m=1}^{M}[D_m R_{mk}] \quad (\mathrm{k}=1, \cdots, N) . \qquad (2)$$

The source strength S_j can then be obtained by solving Eq. (2) under the non-negative condition $S_j \geq 0$.

2.2 Radiation Field and Exposure Estimation

Now that the source strengths have been obtained from Eq. (2), dose rates at any position in the field can be evaluated. This is achieved by substituting the source strengths into Eq. (1) to generate the radiation field and the dose rate contour map. The dose rate D_i at position i is determined by Eq. (1) with S_j obtained from Eq. (2).

Radiation exposure dose is calculated by multiplying the dose rate (D) with the duration of exposure time (T) at the work position. The total dose exposure (E) for a given task can be estimated using the following equation:

$$E = \sum_{i=1}^{L}(D_i \cdot T_{wi}) + \sum_{i=2}^{L}\left[\frac{(D_{i-1}+D_i)}{2} \cdot T_{ti}\right], \qquad (3)$$

where

L = number of working positions,
T_{wi} = work time at position i, and
T_{ti} = travel time between positions i-1 and i.

3. Tracking Simulation

3.1 Test Scene Description

To evaluate the simulation performance of BIMRAD for decommission tracking, a test radiation scene was created by arranging objects within an area of approximate 100 m^2. Fig. 1 illustrates the planar layout of the test scene, displayed with a grid spacing of 1m.

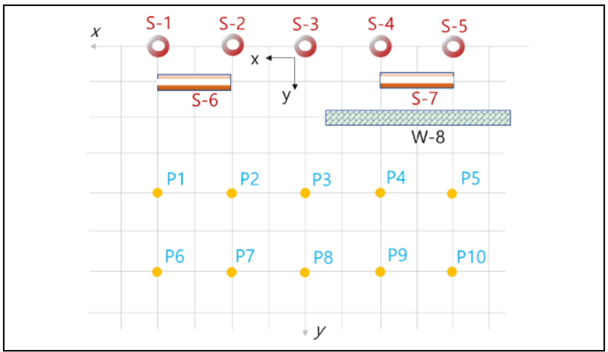

Fig. 1. Planar layout of the test radiation scene.

In Fig. 1, five vertical pipes - with an inner diameter of 10 cm, an outer diameter of 20 cm, and a length of 1 m - were arranged in a row at 2 m intervals along the x-direction. These pipes are centered on the imaginary x-y plane and labeled S-1 through S-5, as depicted in the figure. Additionally, two horizontal transverse pipes, sharing the same diameters and measuring 2 m in length, were placed at the top level of the vertical pipes. These are labeled S-6 and S-7. In total, seven pipes were considered potential sources.

A shielding concrete wall, 20 cm thick and 5 m wide, was positioned on the right side of the area to provide partial shielding for the sources. This wall is labeled W-8.

Ten measurement points were designated on the x-y plane and are identified by their respective numbers in the layout.

Fig. 2 presents the 3D BIM image of the described test scene, generated by BIMRAD. In this image, the seven radiation sources are highlighted in red, the shield wall is displayed in dark green, and the ten measurement points are represented by yellow dots.

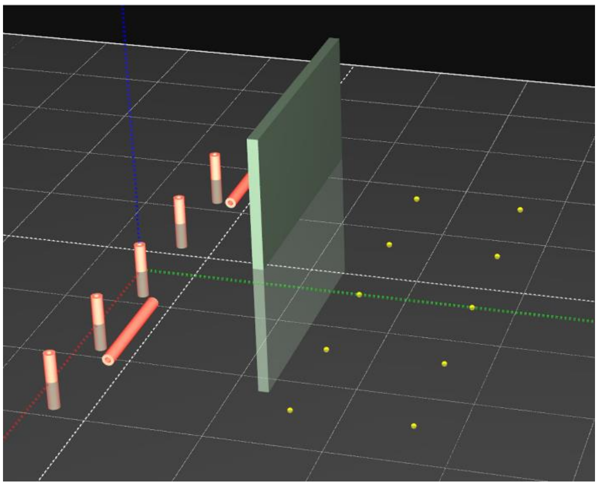

Fig. 2. 3D image of the test scene with the measurement points displayed on an imaginary plane.

3.2 Measured Dose Rates and Source Strength Estimation

Dose rates at the measurement points were calculated using MCNP simulations. The sources were modeled as Co-60 steel, with their strengths arbitrarily assigned within the low-level waste (LLW) range. The source strengths for S-1 through S-7 were set at 3, 5, 8, 10, 20, 5, and 10 MBq/cm³, respectively, with higher strengths assigned to the shielded sources.

Table I presents the dose rates at the 10 measurement points depicted in Fig. 1. These dose rates, corresponding to the specified source strengths, were used as the measured input values for BIMRAD.

Table I: Dose rates at the measurement points.

Meas. Points	**P1**	**P2**	**P3**	**P4**	**P5**
Dose rates ($\mu Sv/hr$)	5299.5	5357.8	3633.9	2273.5	1620.1
Meas. Points	**P6**	**P7**	**P8**	**P9**	**P10**
Dose rates ($\mu Sv/hr$)	2236.9	2117.0	1993.1	1316.5	1056.6

The vertical pipes were modeled as pipe phantoms with 1x4x4 cells in the (r, θ, l) direction, while the horizontal pipes were modeled with 1x4x8 cells.

Table II presents the source strength results estimated by BIMRAD, based on the measured dose rates provided in Table I, compared to the given source strengths. As shown in the table, the estimation error falls within ±40%, which is comparable to the 50% uncertainty recorded in similar applications [5].

Table II: Estimation results of the source strengths.

Sources	**S-1**	**S-2**	**S-3**	**S-4**	**S-5**	**S-6**	**S-7**
Given	3	5	8	10	20	5	10
Estimated	3.11	5.63	11.18	12.92	27.61	5.10	9.08
Error (%)	+3.7	+12.6	+36.7	+29.2	+38.0	+2.1	-9.2

Once the source strengths are determined, the total inventory can be calculated by summing the product of each source strength and the volume of its corresponding source object.

3.3 Construction of the Initial Radiation Field

After the source strengths are determined using Eq. (2), radiation contours can be generated using Eq. (1) for arbitrary positions within the field. While dose rate measurements were initially provided for only a limited number of positions, dose rates are now available for all locations in the field.

Fig. 3 shows the dose rate contour map of the test scene generated by BIMRAD, with the 3400 $\mu Sv/hr$ contour line delineated.

The uncertainty of the evaluated radiation field can be quantified by the errors associated with the re-estimation of the measured values. Table III presents the dose rates re-calculated by BIMRAD at the measurement points, along with the percentage errors relative to the values in Table I. The re-calculated dose rate errors were within ±10% of the measured values. These results are considered highly satisfactory, given that the acceptable uncertainty threshold for industry vendors is 50% [2].

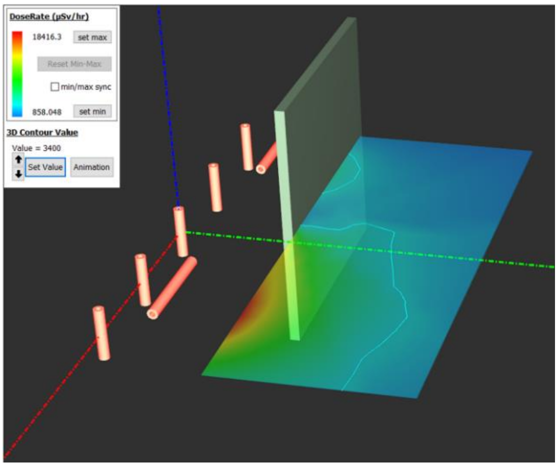

Fig. 3. Radiation contour map of the test scene generated by BIMRAD.

Table III: Re-estimated dose rates and errors to the measured

Meas. Points	P1	P2	P3	P4	P5
Re-calculated ($\mu Sv/hr$)	4850.	5347.	3988.	2499.	1624.
Error (%)	-8.5	-0.20	9.8	10.0	0.25
Meas. Points	P6	P7	P8	P9	P10
Re-calculated ($\mu Sv/hr$)	2150.	2123.	2089.	1449.	1143.
Error (%)	-3.8	0.32	4.8	10.1	8.2

If a radiation task is planned along the path shown in Fig. 4, the estimated radiation exposure from the work is 22,099 μSv. Here, the work time at each point on the path was assumed to be 60 minutes, with no travel time considered between work positions.

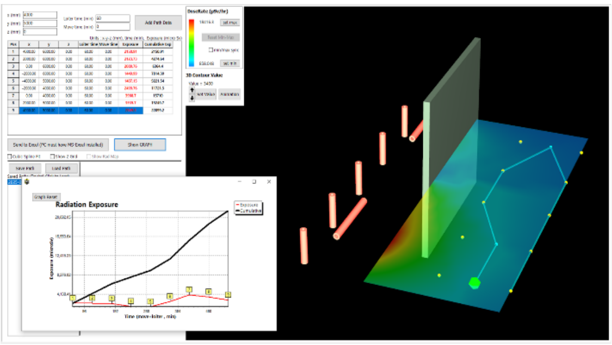

Fig. 4. A radiation work path and the associated radiation exposure graph.

3.4 Dismantling Tracking

As the dismantling of radiation sources progresses, the radiation field undergoes corresponding changes. Fig. 5 provides several snapshots of the source dismantling phases. In these snapshots, the red color of the sources changes to gray when the sources are selected for dismantling. The contour map illustrates the range of dose rates within the designated display area, allowing for a quantitative evaluation of dose rate changes in the radiation field.

It is clearly observable that the area enclosed by the 3,400 $\mu Sv/hr$ contour line diminishes as dismantling progresses. When six sources are dismantled, leaving only one source behind the shielding wall, no areas with dose rates exceeding 3,400 $\mu Sv/hr$ remain. This change in the radiation field can be evaluated without requiring direct dose rate measurements at each dismantling stage.

BIMRAD also offers a three-dimensional contour surface display option. Fig. 6 shows the three-dimensional contour for phase 4 of Fig. 5, with the contour surface representing a dose rate of 1,700 $\mu Sv/hr$.

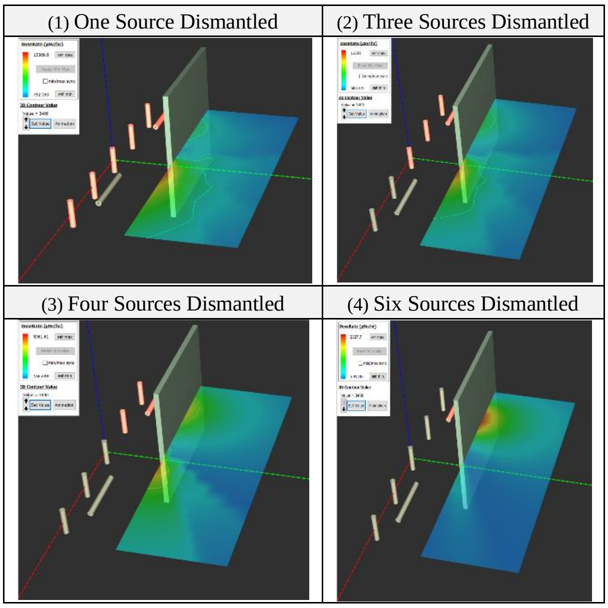

Fig. 5. Radiation field change in accordance with source dismantling.

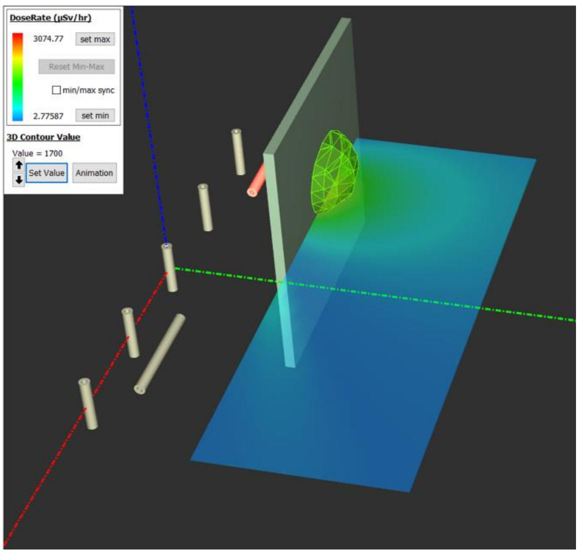

Fig. 6. An example of 3D Radiation contour surface.

BIMRAD can assess the effects of shielding objects. Fig. 7 depicts the radiation contour map generated by BIMRAD when the shielding wall is assumed to be removed in the fourth stage of Fig. 5. In this scenario, the shielding wall changes to dark gray, and the area with a dose rate exceeding 3,400 $\mu Sv/hr$ becomes larger.

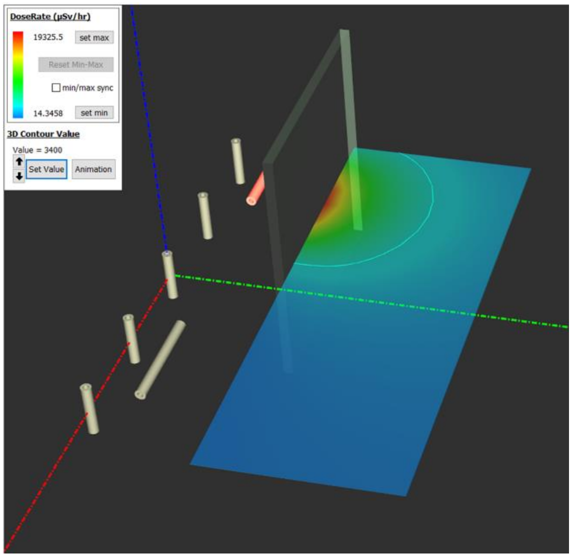

Fig. 7. The radiation contour map when the shielding wall is removed.

Fig. 8 presents the results of radiation exposure evaluations for a work path with the shielding wall and without it. The work path is the same as that in Fig. 4, but now it involves only one radiation source. The estimated radiation exposure from the work is 1,431 μSv when the shielding wall is retained, whereas it increases to 12,319 μSv when the shielding wall is removed.

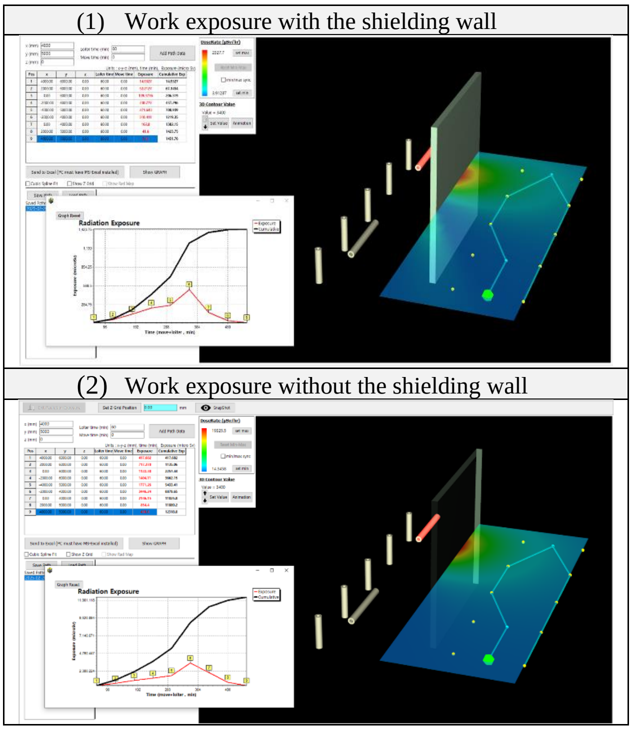

Fig. 8. Comparison of radiation exposures with and without the shielding wall.

4. Conclusions

A BIM-based software tool, called BIMRAD, has been developed to estimate radiation source strengths using field-measured dose rates. This tool is designed to support the estimation of radionuclide inventory distribution within plants, serving as a critical decision-making foundation for NPP decommissioning planning.

BIMRAD also provides 3D dose rate distributions, which are particularly valuable for ALARA analyses in radiation work planning.

The estimation accuracy for source strengths is approximately ±40% for the simulated radiation scene, while the accuracy for dose rates within the radiation field is well within ±20%, as confirmed by BIMRAD's re-estimated results for the measured dose rates. These accuracy levels are considered acceptable, given the comparable industry convention of acceptable uncertainty.

BIMRAD can evaluate dose rate distributions and work exposures across various stages of the dismantling process, while offering 3D visualizations to enhance understanding of the radiation field. This tracking simulation is conducted without requiring additional dose rate measurements at each dismantling stage, once source strengths are determined from initial stage measurements.

The tool can also be utilized to evaluate various alternatives for component dismantling and work planning during NPP decommissioning by leveraging BIMRAD's functionality to either retain or remove sources and shielding objects.

Although the accuracy of the estimations may vary depending on the geometrical complexity of the scene and the precision of dose rate measurements, BIMRAD's methodology is a valuable resource for inventory estimation and exposure analysis during dismantling operations.

ACKNOWLEDGEMENTS

This work was conducted under the project titled 'Development of radiation safety diagnosis platform based on synchronization of digital coordinates and radioactivity information of facilities in NPP' (No. 20217910100130) supported by the Korea Institute of Energy Technology Evaluation and Planning (KETEP) and the Ministry of Trade, Industry and Energy (MOTIE) of the Republic of Korea.

REFERENCES

[1] A. H. Oti, et al., A BIM-driven framework for integrating rules and regulations in the decommissioning of nuclear power plants, Construction Innovation, 22 (4), pp. 809-830, 2022.
[2] P. Tran, Demonstration of Advanced 3D ALARA Planning Prototypes for Dose Reduction, No. 1025310, Electric Power Research Institute, 2012.
[3] SCK•CEN, VISIPLAN 3D ALARA planning and communication tool, https://inis.iaea.org/records/b3dxd-53488, visited in February 2025.

[4] H. C. Kim, et al., A BIM-based Method for Estimating Radiation Source Strengths Using Field-measured Dose Rates, Transactions of the Korean Nuclear Society Autumn Meeting, Gyeongju, Korea, October 26-27, 2023.

[5] H. Toubon, et al., Use of Mathematical Modeling in Nuclear Measurements Projects, 2011 Proceeding 2nd International Conference on Advancements in Nuclear Instrumentation, Measurement Methods and their Applications, Ghent, Belgium, 6-9 June, 2011.